Performance Evaluation of Single-Junction Indoor Photovoltaic Devices for Different Absorber Bandgaps Under Spectrally Varying White Light-Emitting Diodes

Ajanta Saha, K. A. Haque, and Md Zunaid Baten, *Member, IEEE*

Abstract—In this article, we present a detailed theoretical study to predict performance characteristics of single-junction indoor photovoltaic (PV) devices operated under white light emitting diodes (LEDs) having different spectral characteristics. Efficiency limits of both ideal and practical PV converters have been evaluated considering illumination by commercially available white LEDs. The obtained results have been generalized for white LED sources having a wide range of correlated color temperatures (CCTs) and fraction of blue in their corresponding spectrum. Depending on bandgap of the absorber material, both positive and negative correlations are observed between photon conversion efficiency of PV devices and CCT values of the white LED sources. For material bandgaps of ∼1.5 eV or lower, higher photon conversion efficiencies are obtained for warm glow white LEDs. On the contrary, white LEDs characterized to emit cool light are found to be more conducive for PV devices having absorber layer bandgaps of ∼2 eV or higher. The observed characteristics have been explained in terms of linewidth of the main emission peak and relative intensity of blue emission peak of the irradiating white LED spectrum. Based on the analysis of photon yield, three distinct bandgap ranges of the PV absorber material have also been identified, each of which represents different dependence of PV device performances on the white LED spectral characteristics. These results in effect provide the necessary guidelines for designing homojunction, heterojunction, or tandem PV devices suitable for operation under different practical white LED sources.

Index Terms—Correlated color temperature, energy conversion efficiency, indoor photovoltaic (PV), photon yield, red-green-blue (RGB) white light emitting diodes (LEDs).

I. Introduction

CYBERPHYSICAL systems are considered to be the driving force of the fourth industrial revolution–the technological era that is going to be defined by the ubiquity of emerging technologies. Internet of Thing (IOT) devices and systems are at the forefront of these technological break-throughs. Successful operation of cyberphysical systems largely relies on the fidelity of the constituent IOT components, which include wired or wireless communication nodes, sensors, actuators, microcontrollers, and microchips [1], [2]. As the ratings of these low-power electronic devices usually range between few microwatts to several milliwatts, significant efforts are being made to realize microenergy harvesters, which would be able to supplement, if not altogether replace, conventional exhaustible sources of energy supply for IOT and cyberphysical components. Techniques, such as photovoltaic (PV) energy conversion [3], [4], thermoelectric generation [5], and motion-based energy harvesting [6] have already been proposed and studied in this regard. Energy scavenging from indoor light sources is considered to be the most prospective among these techniques, primarily because of the maturity and proven track-record of the PV energy conversion technology and also because of recent advancements of the solid-state lighting industry [7]–[9].

The viability of harvesting indoor ambient light by means of PV energy converters have been studied extensively over the recent years. Research in this area has primarily focused on designing and realizing indoor PV (IPV) devices based on different material systems, such as silicon [10]–[12], CIS, CIGS [13], CZTSSe [14], GaAs, GaInP [15], [16], CdTe [17], organics [18], dye-sensitized materials [19], and perovskites [20]. Indoor illumination from different light sources, such as white LED, halogen lamp, incandescent lamp, sodium discharge lamp, and fluorescent lamp have been considered in these studies. However, an aspect that has been rather overlooked in evaluating the performance of IPV devices, is the detailed understanding of how their performance characteristics are influenced by the fine spectral features of the illuminating light source. The red-green-blue (RGB) white LED deserves particular attention in this regard because of the wide spread commercial usage of these highly efficient and reliable light sources. Though a maximum efficiency limit of 60% has been estimated for the ideal PV converter when illuminated by a typical white LED source [21], it remains to be seen how white LEDs having different spectral characteristics influence the energy conversion efficiency of different IPV converters.

In this article, we present a systematic study to establish the correlation between energy conversion efficiency of single-junction IPV converters and spectral characteristics of RGB white LED sources. Maximum efficiency limits of ideal PV converters are evaluated considering radiation from commercially available white LEDs having spectrally different characteristics. As a test case for a practical device, performance characteristics of the reported highest efficiency CZTSSe solar cell is evaluated by numerically solving Poisson's equation and continuity equation under optical generation-recombination conditions considering illumination by these white LED sources. The findings are further generalized for ideal PV converters of different material bandgaps, considering operation under white LED sources having different correlated color temperatures, emission linewidths and relative intensity of blue. The results of the analysis indicate that depending on the relation between PV material bandgap and photon yield corresponding to the illuminating spectrum, the conversion efficiency of a PV device can be negatively or positively correlated with spectral characteristics of the white LED source. The results in effect provide guidelines for designing efficient and reliable PV devices for operation under practical white LED sources.

II. CHARACTERIZATION UNDER PRACTICAL INDOOR SPECTRA

To evaluate performance characteristics of PV energy converters under typical indoor lighting conditions, several commercially available white LED sources have been considered in this article [22]. Spectral power distribution [$S(\lambda)$] of these light sources are shown in Fig. 1(a). The CIE 1931 color space chromaticity diagram and calculated color temperatures for these spectra are depicted in Fig. 1(b) (see supporting information for details). As can be seen, correlated color temperature (CCT) values of the LEDs vary from 2308 K (warm glow) to 5833 K (cool white), which is basically the effective range of color temperature of typically available commercial white LEDs. In order to estimate maximum conversion efficiency of an ideal PV converter under these practical light sources, Shockley–Queisser limits are calculated as per Green's approximation [21]. As shown in Fig. 2(a), the peak efficiency limit for different bandgaps of the PV absorber material vary from 58%–68% over an optimal bandgap range of 1.7–1.9 eV. These values are significantly higher than the maximum efficiency limit of 34% obtainable under AM1.5 solar irradiation. Such high values of efficiency limit can be explained in terms of the corresponding photon yield, which is defined as

$$\text{Photon Yield} = \int_0^{\lambda_g} \Phi(\lambda) \ d\lambda. \tag{1}$$

Here, $\Phi(\lambda)$ is the spectral photon flux of the considered light source and $\lambda_g = hc/E_g$, where E_g is the bandgap of the PV absorber material, h is Planck's constant and c is the vacuum speed of light. The calculated photon yields for the white LED sources and also for AM1.5 solar spectrum are plotted in Fig. 2(b). It is to be noted that for comparing photon yield, intensity of each spectrum was scaled such that the total power density remains constant at 1000 W/m^2. As can be observed
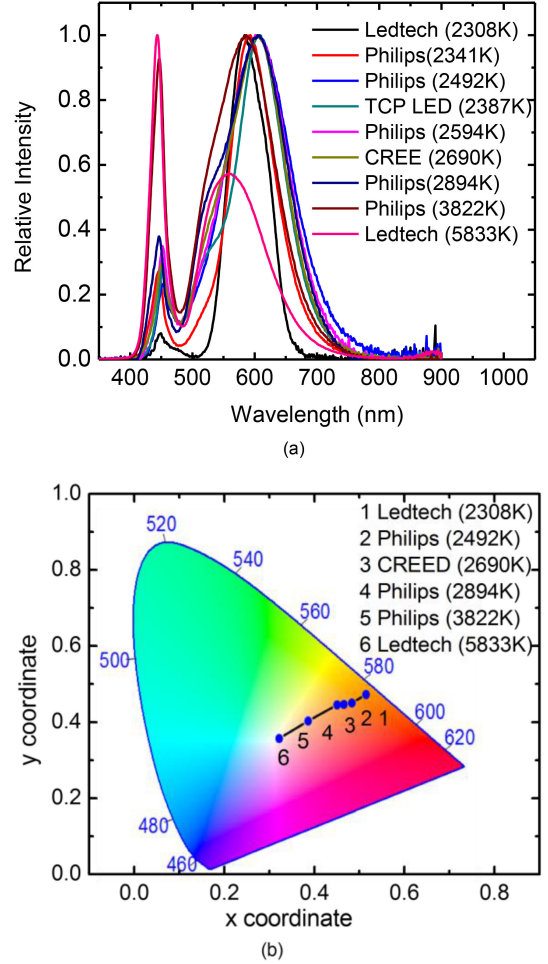
Fig. 1. (a) Spectral power distribution. (b) CIE 1931 chromaticity diagram with chromaticity coordinates of commercial white LED sources (CCT values shown in parentheses).

in Fig. 2(b), for the entire range of bandgap, percentage of light absorbed by an ideal PV converter is much higher under a white LED source, than under solar radiation. It is also quite obvious that photon yield values obtained for different LEDs vary significantly depending on CCT of the illuminating spectra and bandgap of the PV absorber material, thereby indicating a possible correlation between the two.

To further investigate a PV device's performance under white LED sources having different CCTs, a practical CZTSSe-based thin film device is considered. This device was previously reported to have demonstrated the record efficiency value of 12.6% under solar irradiation [23] and a theoretical efficiency value of 13.77% under typical white LED illumination [14]. Detailed heterostructure and layer thicknesses of the considered CZTSSe device are described in Supporting Information. To evaluate performance of this device under different white LED sources, a theoretical model based on numerical solution of Poisson's equation and continuity equation under optical generation-recombination conditions is considered (see supporting information for details). The conversion efficiencies obtained using this model, along with CCT values of the illuminating white LED sources are

This article has been accepted for inclusion in a future issue of this journal. Content is final as presented, with the exception of pagination.

SAHA *et al.*: PERFORMANCE EVALUATION OF SINGLE-JUNCTION INDOOR PHOTOVOLTAIC DEVICES 3
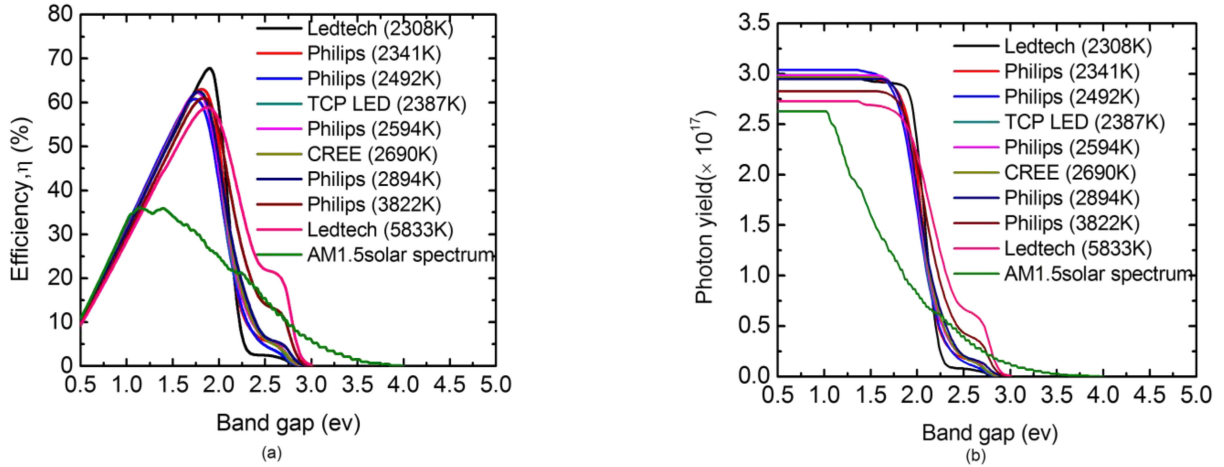
Fig. 2. (a) Limiting Shockley–Queisser efficiency of an ideal PV converter as a function of material bandgap. (b) Photon yield as a function of bandgap for different commercial white LED sources and AM 1.5 solar radiation.

TABLE I
LED SOURCES WITH THEIR CCTS AND CORRESPONDING
EFFICIENCIES OF THE CZTSSE DEVICE

White LED source	CCT(K) of the LED	Efficiency of the CZTSSe device, η (%)
Ledtech Bridgelux	2308	14.61
Philips Streetview	2341	14.77
TCP LED PAR20	2387	14.8
Philips LED A19	2492	14.98
Philips LED Candle Light	2594	14.81
CREE LED BR30	2690	14.8
Philips LED PAR20 Flood	2894	14.68
Philips LED 3white-board	3822	14.14
Ledtech LED PAR20	5833	13.55

given in Table I. As can be observed, the efficiency values obtained under different white LED sources vary from 13.55% to 14.98%. A comparative picture is presented in Fig. 3(a), which shows the relative efficiency enhancement obtained by taking the lowest efficiency value of Table I as the reference. The observed trend is in fact very much in accordance with the photon yield versus CCT characteristics of this device which is also plotted in Fig. 3(a). This indicates that photon yield can describe how a specific PV converter's efficiency can vary depending on CCT value of the white LED source. However for a generalized description, CCT of the white LED source needs to be correlated with the conversion efficiencies of PV converters having different material bandgaps. In Fig. 3(b), the maximum efficiency limit for different material systems are calculated and plotted as a function of CCT values of these practical white LED sources. As can be observed, for different CCTs of the white LED source, efficiency of single-junction PV devices can vary by about 3.8% to 9.5% depending on absorber material.

III. GENERALIZED DESCRIPTION BASED ON THEORETICALLY MODELED SPECTRA

In order to generalize the observed behavior of the PV converter under different white LED sources, reference spectra are systematically generated such that they correspond to CCT values ranging from 2220 to 5850 K. It is important to note that CCT of a white LED source may vary depending on two factors, namely the variation of relative intensity of the blue emission peak (I_B) and the variation of linewidth ($\Delta\lambda$) of the broader emission centered at 600 nm. To account for both these factors, two different sets of LED spectra have been generated and considered. For the first set of spectra [see Fig. 4(a)], peak intensity of blue emission is increased from 2% to 150% of the main emission peak by keeping $\Delta\lambda$ unchanged, thereby resulting in CCT variation from 2420 to 5850 K. The second set of spectra in Fig. 4(b) are generated by varying $\Delta\lambda$ from 90 to 550 nm while keeping peak blue emission intensity constant, thereby resulting in CCT values ranging from 2220 to 5213 K. To have an estimate of the fraction of light absorbed by an ideal PV converter under these spectra, photon yields are calculated and plotted in Fig. 5(a). As can be observed, for all the spectra the photon yield (PY) remains invariant with bandgap as it varies from 0.5 to 1.6 eV. However, PY decreases sharply for material bandgaps residing between 1.6 and 2.25 eV, and then decreases at a less steep slope for bandgaps larger than 2.25 eV. Based on these observations, three characteristic regimes labeled as regions I, II, and III, have been identified in Fig. 5(a).

To establish the general relation between PY and CCT in these three regimes, photon yields are next calculated for different bandgaps of the PV absorber material. For Region I, a material bandgap of 1.5 eV is considered and the corresponding photon yields are calculated and plotted for LEDs having different CCT values. As shown in Fig. 5(b), both positive and negative correlations are obtained between PY and CCT, depending on whether $\Delta\lambda$ or I_B is increasing.

This behavior is better explained with respect to the fraction of blue in the corresponding spectrum, which actually increases

This article has been accepted for inclusion in a future issue of this journal. Content is final as presented, with the exception of pagination.

4

IEEE JOURNAL OF PHOTOVOLTAICS
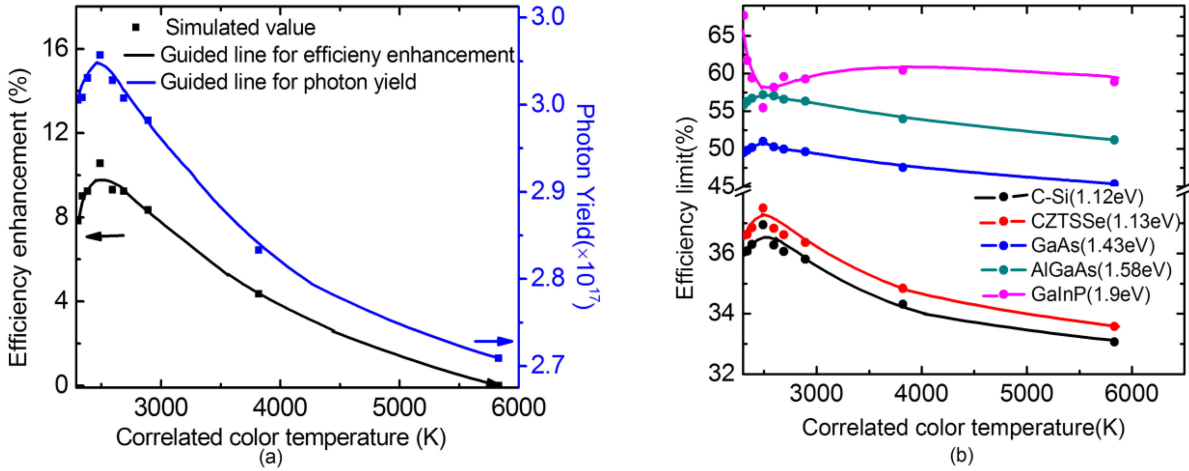
Fig. 3. (a) Relative enhancement of efficiency taking the lowest efficiency as reference and calculated photon yield for the CZTSSe device. (b) Limiting Shockley–Queisser efficiency of an ideal PV converter of different absorber materials (bandgaps shown in parentheses) as a function of CCT of the commercial LED sources.
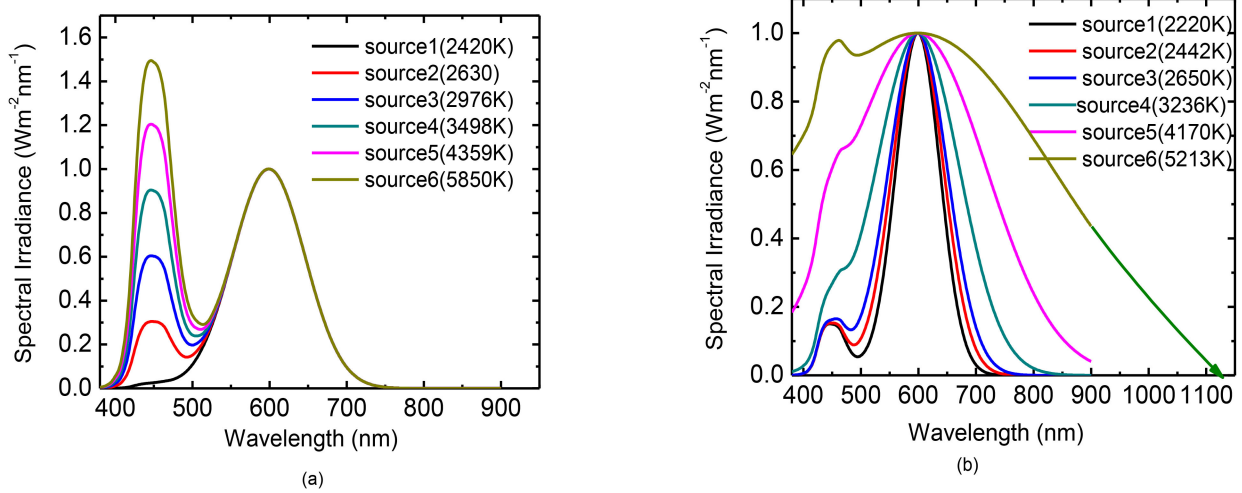
Fig. 4. Spectral Irradiance of reference spectra (CCT values shown in parentheses) generated (a) by varying peak intensity of blue emission while keeping main emission linewidth constant and (b) by varying linewidth of main emission while keeping peak intensity of blue emission constant.

both with the increase of I_B and decrease of $\Delta\lambda$. As the blue emission corresponds to a relatively high energy of the incident photon, an increase in the fraction of blue effectively reduces the number of photons per unit energy, thereby reducing the overall photon flux that can be absorbed by the PV device. The solid line shown in Fig. 5(b) represents the PY versus CCT characteristics expected for the commercial white LED spectra considered in this article. It is noteworthy that this trend is qualitatively similar to the previously obtained PY versus CCT characteristics [see Fig. 3(a)] of the CZTSSe device, for which the absorber layer bandgap was 1.1 eV. Because PY is independent of bandgap in region I, similar characteristics are expected for PV converters having any other material bandgap within this region. This is evident from Fig. 3(b) also, which shows similar qualitative dependence of efficiency limits on CCT for CZTSSe, AlGaAs, crystalline silicon(c-Si), and GaAs materials, all of which have bandgaps within region I.

The dependence of photon yield on the illuminating spectrum is further illustrated in Fig. 5(c) and (d) for material bandgaps corresponding to regions II and III, respectively. The solid lines shown in these figures indicate the characteristics expected from operation under commercial white LED sources. For materials of high bandgap, the photon conversion efficiency, and hence the photon yield is expected to increase if there is an increase in the number of higher energy photons in the incident spectrum. Therefor enhancement of the percentage of blue in the white LED source, resulting from either increase of I_B or decrease of $\Delta\lambda$, should increase the photon yield for materials of high bandgap. Such a trend is particularly evident in Region III, where material bandgaps ranging from 2.5 to 3 eV can absorb only the high energy photons residing in the vicinity of the blue region of the emission spectrum. Consequently for material bandgaps of 2.5 eV or higher, PY tends to increase as the illuminating source tend to be more cool white in nature. Based on the choice of

This article has been accepted for inclusion in a future issue of this journal. Content is final as presented, with the exception of pagination.

SAHA *et al.*: PERFORMANCE EVALUATION OF SINGLE-JUNCTION INDOOR PHOTOVOLTAIC DEVICES 5
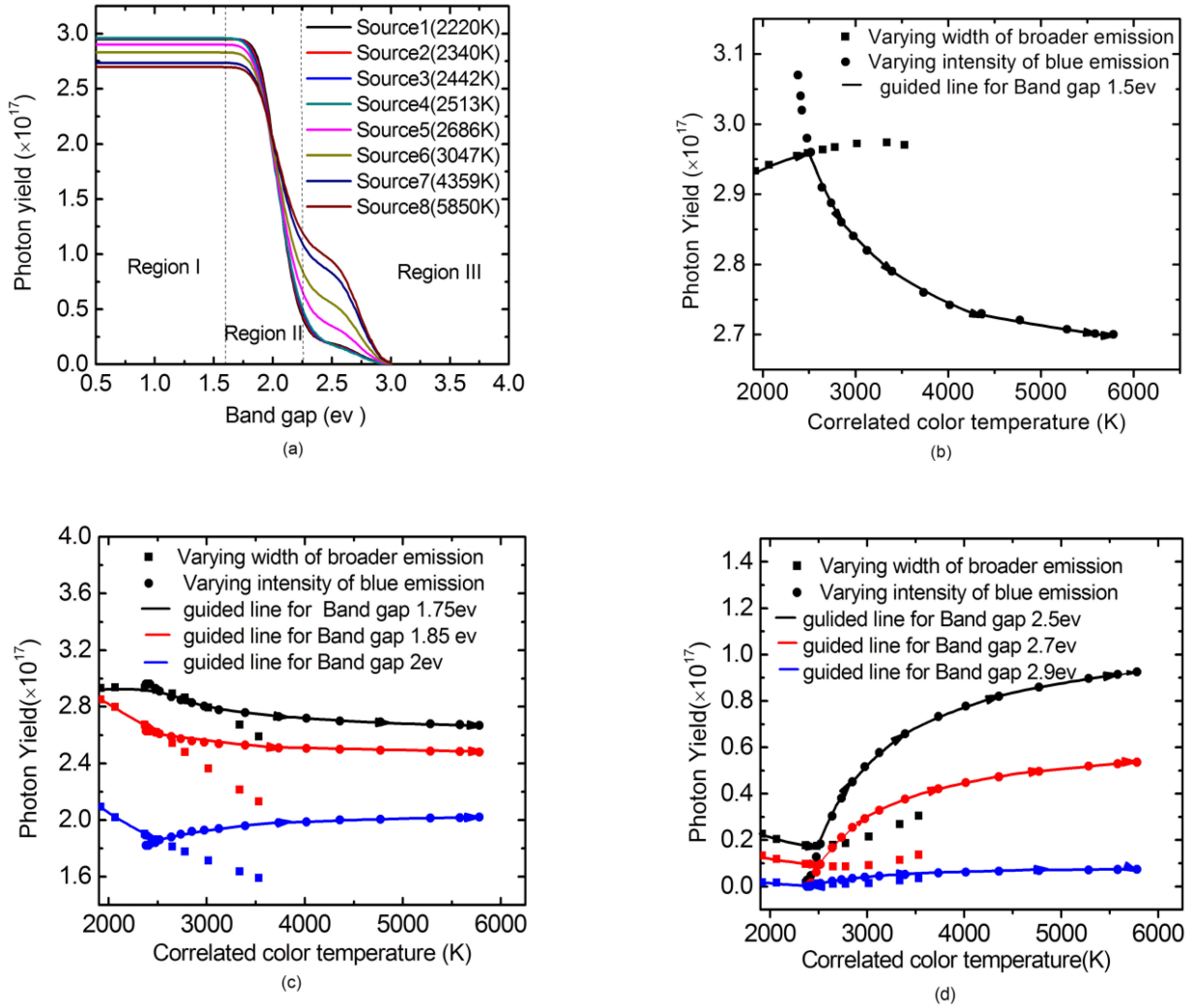
Fig. 5. (a) Photon yield as a function of material bandgap for the generated reference set of spectra having intensity of 1000 W/m^2; photon yield versus CCT characteristics for different material bandgaps representing (b) region I, (c) region II, and (d) region III [circle and square for spectra of Fig. 4(a) and (b), respectively, and solid line for expected commercial white LED spectra].

material bandgap in Region II, the dependence of PY on CCT exhibits characteristics similar to those of Region I or III. As has been shown by the solid line in Fig. 5(c), for a relatively smaller bandgap of 1.75 eV, PY tends to remain nearly invariant with CCT for up to 2500 K and then decrease monotonically as CCT further increases, a characteristic similar to that of region I. On the contrary, for higher values of bandgap, such as for $E_g = 2$ eV as has been considered in the plot, the trend appears to be in accordance with the characteristics observed in region III. It is noteworthy that in the efficiency limit versus CCT plot of Fig. 3(b), similar characteristic trend is obtained with GaInP, for which a material bandgap of 1.9 eV is considered.

A summary of the results obtained for the three regions is illustrated using false color plots in Fig. 6. The color plots shown in Figs. 6(a)–(c) present the dependence of PY on I_B and $\Delta\lambda$, for specific bandgaps of the PV absorber material representing regions I–III, respectively. As can be observed, low linewidth of the main emission peak of the white LED source is preferred for all bandgaps of the PV absorber material in order

to attain high photon yields. On the other hand, high intensity of the blue emission peak is desirable for the PV materials having bandgaps of 2 eV or higher. The relation of PY with material bandgap and CCT is shown in Fig. 6(d), which clearly illustrates the three regions signifying the dependence of photon conversion efficiency on CCT of the illuminating spectra. The results shown here indicate that for absorber materials having bandgaps smaller than 2 eV, higher photon conversion efficiency is expected for operation under warm glow white LEDs. On the contrary, white LEDs emitting cool light are more suitable for PV converters designed with higher bandgap absorber materials.

These results, therefore, provide the guidelines for designing homojunction, heterojunction or tandem PV devices suitable for operation under white LED sources having different spectral characteristics. These design considerations are expected to be unavoidable for realizing practical indoor PV devices which can efficiently and reliably operate as integral components of future cyberphysical systems.

This article has been accepted for inclusion in a future issue of this journal. Content is final as presented, with the exception of pagination.

6   IEEE JOURNAL OF PHOTOVOLTAICS
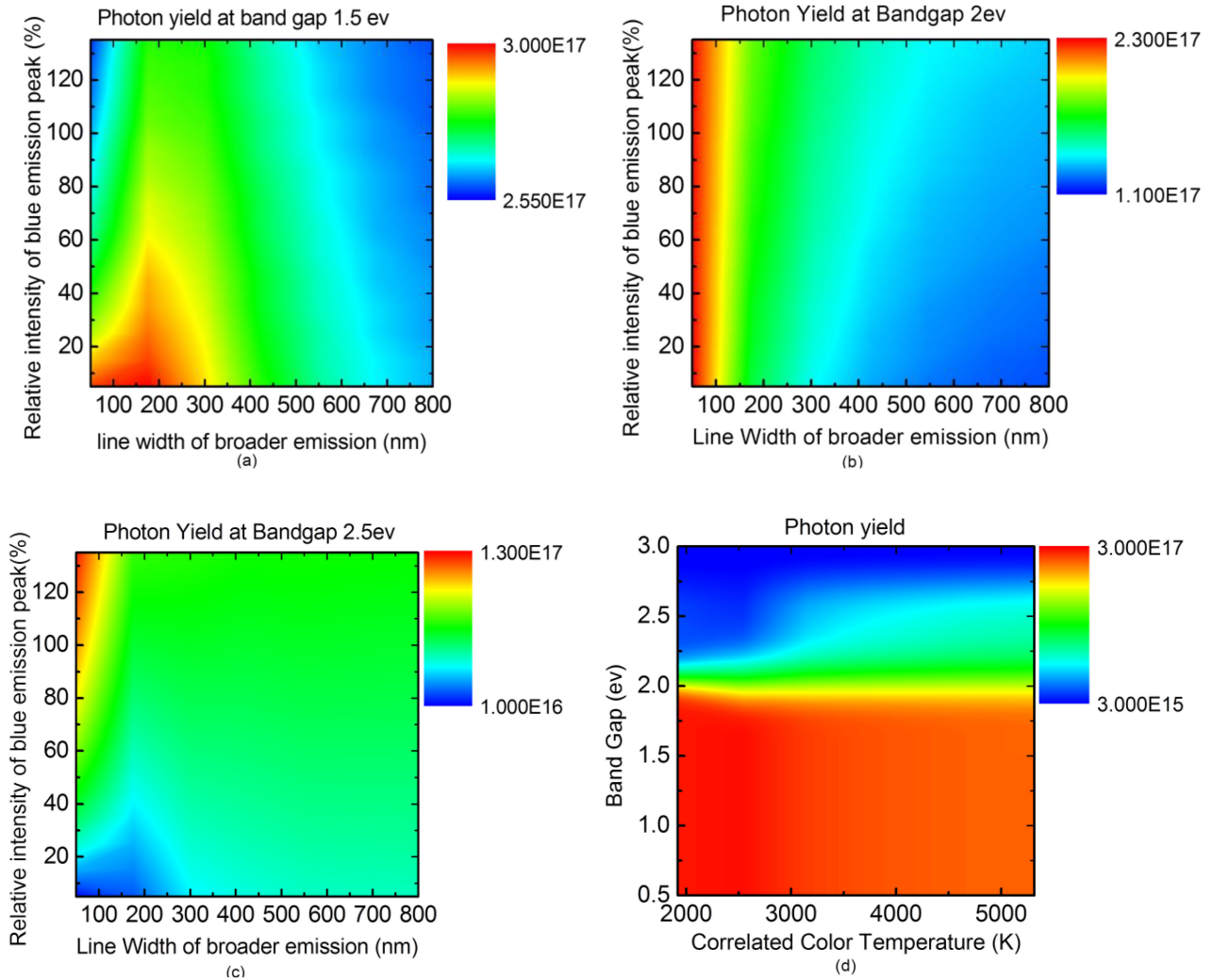
Fig. 6. Photon yield as a function of main emission peak's linewidth and blue emission peak's intensity of reference spectra(intensity 1000 W/m^2) for absorbing material of (a) band gap 1.5 ev, (b) band gap 2 ev, (c) band gap 2.5 ev, and (d) photon yield as a function of spectra's CCT and band gap of the absorbing material.

IV. CONCLUSION

The dependence of PV energy conversion efficiency on spectral characteristics of the illuminating white LED source has been studied in detail in this article. Considering illumination by different commercially available white LED sources, energy conversion efficiency of an experimentally reported CZTSSe device is estimated based on numerical simulation of Poisson's and continuity equations under optical generation-recombination conditions. For a specific absorber material, the obtained characteristics are found to be intricately related to the correlation between color temperature and photon yield of the illuminating spectrum. The findings have been further generalized for any combination of PV absorber material and white LED spectrum of interest. The established general framework between conversion efficiency of the indoor PV device and correlated color temperature of the illuminating spectrum indicate that depending on bandgap of the PV absorber material and fraction of blue of the white LED spectrum, both positive and negative correlations are possible between energy conversion efficiency of the PV device

and CCT of the white LED source, whereas warm glow white LEDs are found to be more conducive for material bandgaps of 1.5 eV or smaller, cool white emitting LEDs should be favored for higher bandgap materials to attain higher conversion efficiencies. The results presented here therefore provide necessary guidelines for designing spectra dependent energy harvesters suitable for operation under practical solid-state light sources.

REFERENCES

[1] A. Tzounis, N. Katsoulas, T. Bartzanas, and C. Kittas, "Internet of Things in agriculture, recent advances and future challenges," *Biosyst. Eng.*, vol. 164, pp. 31–48, 2017.

[2] J. Lee, B. Bagheri, and H. A. Kao, "A cyber-physical systems architecture for Industry 4.0-based manufacturing systems," *Manuf. Lett.*, vol. 3, pp. 18–23, 2015.

[3] A. Nasiri *et al.*, "Indoor power harvesting using photovoltaic cells for low-power applications," *IEEE Trans. Ind. Electron.*, vol. 56, no. 11, pp. 4502–4509, Nov. 2009.

[4] H. Yu, "Power management and energy harvesting for indoor photovoltaic cells system," in *Proc. 2nd Int. Conf. Mech. Autom. Control Eng.*, 2011, pp. 521–524.

This article has been accepted for inclusion in a future issue of this journal. Content is final as presented, with the exception of pagination.

SAHA *et al.*: PERFORMANCE EVALUATION OF SINGLE-JUNCTION INDOOR PHOTOVOLTAIC DEVICES 7

[5] J. P. Carmo, L. M. Gonçalves, and J. H. Correia, "Thermoelectric microconverter for energy harvesting systems," *IEEE Trans. Ind. Electron.*, vol. 57, no. 3, pp. 861–867, Mar. 2010.

[6] H. Fang *et al.*, "Fabrication and performance of MEMS-based piezoelectric power generator for vibration energy harvesting," *Microelectron. J.*, vol. 37, pp. 1280–1284, 2006.

[7] M. S. Shur and A. Žukauskas, "Solid-state lighting: Toward superior illumination," *Proc. IEEE*, vol. 93, no. 10, pp. 1691–1703, Oct. 2005.

[8] E. F. Schubert and J. K. Kim, "Solid-state light sources getting smart," *Science*, vol. 308, no. 5726, pp. 1274–1278, Oct. 2005.

[9] J. Cho, J. H. Park, J. K. Kim, and E. F. Schubert, "White light-emitting diodes: History, progress, and future," *Laser Photon. Rev.*, vol. 11, no. 2, 2017.

[10] N. H. Reich, W. G. J. H. M. van Sark, and W. C. Turkenburg, "Charge yield potential of indoor-operated solar cells incorporated into Product Integrated Photovoltaic (PIPV)," *Renew. Energy*, vol. 36, no. 2, pp. 642–647, 2011.

[11] H. Águas *et al.*, "Thin film silicon photovoltaic cells on paper for flexible indoor applications," *Adv. Funct. Mater.*, vol. 25, no. 23, pp. 3592–3598, 2015.

[12] S. W. Glunz *et al.*, "High-efficiency silicon solar cells for low-illumination applications," in *Proc. Conf. Rec. 29th IEEE Photovolt. Specialists Conf.*, New Orleans, LA, USA, 2002, pp. 450–453.

[13] B. Minnaert and P. Veelaert, "Efficiency simulations of thin film chalcogenide photovoltaic cells for different indoor lighting conditions," *Thin Solid Films*, vol. 519, no. 21, pp. 7537–7540, 2011.

[14] K. A. Haque and M. Z. Baten, "On the prospect of CZTSSe-based thin film solar cells for indoor photovoltaic applications: A simulation study," *AIP Adv.*, vol. 9, no. 5, p. 055326, 2019.

[15] A. S. Teran *et al.*, "AlGaAs photovoltaics for indoor energy harvesting in mm-scale wireless sensor nodes," *IEEE Trans. Electron Devices*, vol. 62, no. 7, pp. 2170–2175, Jul. 2015.

[16] I. Mathews, P. J. King, F. Stafford, and R. Frizzell, "Performance of III–V solar cells as indoor light energy harvesters," *IEEE J. Photovolt.*, vol. 6, no. 1, pp. 230–235, Jan. 2016.

[17] K. Shen *et al.*, "CdTe solar cell performance under low-intensity light irradiance," *Sol. Energy Mater. Solar Cells*, vol. 144, pp. 472–480, 2016.

[18] H. K. H. Lee *et al.*, "Organic photovoltaic cells-promising indoor light harvesters for self-sustainable electronics," *J. Mater. Chem. A*, vol. 6, no. 14, pp. 5618–5626, 2018.

[19] M. Freitag *et al.*, "Dye-sensitized solar cells for efficient power generation under ambient lighting," *Nat. Photon.*, vol. 11, no. 6, pp. 372–378, 2017.

[20] G. Lucarelli *et al.*, "Efficient light harvesting from flexible perovskite solar cells under indoor white light-emitting diode illumination," *Nano Res.*, vol. 10, no. 6, pp. 2130–2145, 2017.

[21] M. F. Müller, M. Freunek, and L. M. Reindl, "Maximum efficiencies of indoor photovoltaic devices," *IEEE J. Photovolt.*, vol. 3, no. 1, pp. 59–64, Jan. 2013.

[22] "LSPDD: Lamp spectral power distribution database," 2016. [Online]. Available: http://galileo.graphycs.cegepsherbrooke.qc.ca/app/en/home, Accessed on: Feb. 22, 2019.

[23] W. Wang *et al.*, "Device characteristics of CZTSSe thin-film solar cells with 12.6% efficiency," *Adv. Energy Mater.*, vol. 4, no. 7, pp. 1–5, 2014.